Effect of Externally Applied Liquid Pressure on Wicking in Paper Wipes

Reza Masoodi[1], Ph.D., Krishna M. Pillai[1], Ph.D., and Padma P. Varanasi[2], Ph.D.

[1]Laboratory for Flow and Transport Studies in Porous Media

University of Wisconsin-Milwaukee, Milwaukee, WI, USA

[2]Waukesha Electric Systems, Waukesha, WI, USA

Correspondence to:

Krishna M. Pillai at: krishna@uwm.edu

ABSTRACT

Wicking of liquid under externally applied liquid pressure into three paper wipes is studied for the first time. Darcy's law and capillary-tube flow form the basis of two separate theoretical models which were tested through experiments. The wicking and wetting parameters of the tested wipes were measured independently to enable such a comparison without the use of any fitting parameters. Darcy model is found to work better under zero hydraulic pressure, i.e. pure wicking; however capillary model is more accurate when the incoming liquid is pressurized. An increase in the applied pressure led to an increase in the liquid absorption rate and a decrease in the saturation time. However, its relative effect on the absorption rate and saturation time was found to decrease with an increase in its magnitude.

INTRODUCTION

Wicking is the spontaneous imbibition of liquid into a porous medium where the driving force that pulls the liquid into the medium is the capillary suction force. This suction force arises as a result of wetting of pore surfaces in a porous medium by the moving liquid-front. Sometimes other types of forces such as gravity or hydraulic force at the entrance may act as drivers in the wicking of liquids in porous media. Previous research on wicking can be classified into two categories: a) Study of the relation between the wicking rate, and the wicking and wetting parameters. b) Study of the experimental methods for measuring wicking and wetting parameters.

Lucas [1], Washburn [2], and Poiseuille [3] were the first researchers who studied the relation between the wicking rate and time. They reported a linear relation between the wicking rate and the square root of time, i.e., $L^2 = k_0 t$ in which L is wicked mass or height of the column of liquid wicked into the porous medium. In the first mathematical models proposed for the wicking process, the inertial and gravitational forces were not considered in the models. These assumptions resulted in a simple model called the Washburn equation for the theoretical prediction of the wicking process. Szekely et al. [4] added the inertial and gravity forces to the previous models and developed an accurate differential equation for the wicking rate.

Darcy [5] developed a simple formula that related the velocity of a liquid to its pressure drop within the porous medium. Pillai et al. tried to study the restrictions of the Darcy's law and Washburn equation, and modified them for modeling fluid motion in certain types of porous media [6,7].

Several researchers have studied the relation between the wicking rate and the porous medium characteristics. The wicking rate along fibers was first studied by Chwastiak [8], Scher [9], and Hodgson and Berg [10]. Others such as Fowkes [11], Williams et al. [12], and Pillai and Advani [6] studied the wicking rate across the fibers. Kim et al. [13] studied experimentally the dependence of sorption of fibrous assemblies on their structure and fabrication. Masoodi et al. [7] developed a new formula for capillary force when the porous media is composed of sphere-like beads of a certain size distribution. Masoodi et al. [14] studied the effect of the hydraulic and capillary radii on the wicking rate into the wipes. A complete review of the research on wicking can be found in Chatterjee and Gupta [15], and in Pan and Gibson[16].

Zhong et al[17,18] tried to use the statistics based Ising model to simulate the wetting and fluid transport in fibrous materials. The 3-D version of

their model was used by Lukas et al. [19] to numerically simulate the liquid transport in fibrous materials. Their model is not as simple as the traditional wetting models and can only be solved numerically. More details on the Ising model can be found in work by Patniak et al. [20], and Pan and Zhong [21].

Wetting is an initial requirement for wicking. The parameter that indicates the wettability of any surface is the contact angle, which is the angle between the tangent lines of the liquid-air and solid-liquid interfaces at the liquid front within the porous medium. The wetting phenomenon was first studied by T. Young [22] and Gauss [23]; they concluded that the contact angle is a function of the surface energies of both liquid and porous matrix. Literature in the fields of dynamic and static contact angle was reviewed by Dussan and Davis [24], and Dussan [25]. Although several researchers proposed mathematical equations for predicting the contact angle, however such formulas are very restrictive and researchers prefer to measure the contact angle rather than use mathematical formulas to predict them.

Wicking parameters such as pore size and contact angle are very important in the modeling of liquid transport into porous media. A comprehensive review of experimental techniques for measuring the wetting and wicking parameters was done by Ghali et al [26]. Li et al [27] used the wicking techniques for measuring the pore size in ceramic materials where they used low energy liquids to ensure zero contact angle. After estimating the pore radius, they used the same technique to measure the contact angle as well. Bachmann et al. [28] used the Wilhelmy plate method (WPM) and the modified capillary rise method (MCRM) for measuring contact angle and particle surface energy in porous media. A well-established method for determination of pore size distribution in a porous medium is the method of mercury porosimetry [29] where the mercury is made to penetrate into a porous medium under pressure. The surface energy of mercury is very high, which leads its contact angle to be more than 90 degrees in most cases, so a high external pressure needs to be applied on the invading liquid to drive the mercury into porous medium. Dang-vu and Hupka [30] used the capillary rise method to measure the contact angle and pore size for different porous media.

Absorption or wicking rate is the most important characteristic studied in the literature on absorbing technology [15]. When someone uses a stationary wipe to absorb liquid laid on a surface, the only driving force for wicking comes from the capillary pressure. However if somebody uses a wipe to clean a wet surface by moving the wipe over the surface, due to the forcing of liquid into the wedge created by the wipe and the surface, an extra hydrodynamic pressure in the wedge along with the capillary pressure inside the wipe drive the liquid absorption. This extra pressure facilitates the

a) A photo of the testing setup

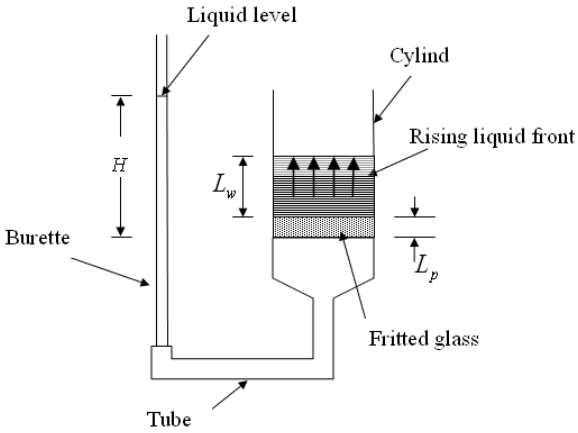

b) A schematic of the testing setup

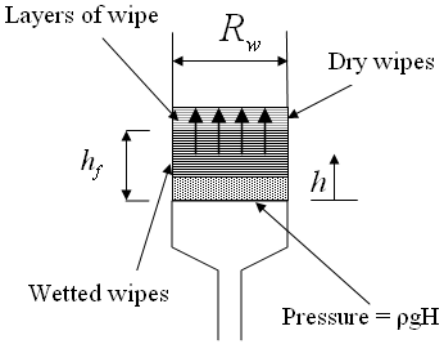

c) Details near the flow-front inside the stack of wipes

FIGURE 1. A schematic and photo of the testing setup used to study the effect of externally imposed liquid-pressure on the wicking rate in a wipe-stack.

absorption and increases the wicking speed—we will refer to such a pressure as the external pressure. As is evident from the literature survey described above, no previous study has evaluated the effect of external pressure on wicking rate in paper wipes. We plan to study the wicking of liquid into ordinary paper wipes under an externally applied liquid pressure where we will compare the experimental results with the predictions of two theoretical models based on the capillary-tube and Darcy's-law based flows. Different wicking parameters used in the two models are to be measured independently in this study. Liquid absorption as a function of time as well as the time taken for a given volume of liquid to wick into the wipes are to be studied.

a) The layers of wipes stacked in the cylinder

b) The tool that was used to cut the wipes

FIGURE 2. The detail of cutting paper wipes and stacking layers in the cylinder

Figure 1 shows a photo and a schematic of our test setup where a liquid column was used to create an externally applied liquid pressure at the bottom of a stack of wipes. Changing the height of the liquid column enabled us to study the effect of varying externally applied liquid pressure on wicking in the stack of wipes. Paper wipes, which have cellulose as their main constituent and which are commonly used in the household, medical and industrial applications, were used in this study. Layers of paper towel or table napkin were stacked on top of a 'fritted glass' (a porous screen) in the cylinder (see *Figure 2*). The rate of reduction of liquid level in the burette was measured using a digital camera. Each film was reviewed several times to extract the exact position of the liquid level at different times during the wicking process. As the volume of liquid employed for wetting the stack of wipes was very small, changes in external pressure, which is related to the height of liquid column in the burette, could be neglected during the wipe-saturation process.

MATHEMATICAL DESCRIPTION OF WICKING MODELS

As we reviewed in the introduction, there are essentially two conventional models that are popular in wicking studies: the Washburn model and the Darcy's law based model. We will use both of these two models to compare our experimental results with theoretical predictions.

Capillary Model

We assume our porous medium created by wipes to be equivalent to a bundle of vertically aligned capillary tubes. The energy balance equation for liquid flow within the capillaries can be written as

$$\frac{p_0}{\rho g}+\frac{u_0^2}{2g}+h_0=\frac{p_f}{\rho g}+\frac{u_f^2}{2g}+h_f+h_L \qquad (1)$$

where h is the vertical coordinate in the porous medium, p is the pressure, u is the average velocity of fluid within a capillary tube, and h_L is the head loss. Subscript 0 indicates the initial value of each parameter and subscript f indicates the value of parameters at the liquid front. Note that h_f is the length of the capillary tube filled with the liquid. Since the velocity is purely axial and constant in the capillary tubes (i.e. u_0=u_f.), Eq. (1) can be expressed as

$$p_0-p_f=\rho g h_f+\rho g h_L \qquad (2)$$

after recognizing that $h_0=0$. The pressure terms in Eq. (2) can be obtained through boundary conditions on the fluid as

$$p_0=p(h=0)=p_h+p_{atm} \qquad (3a)$$

$$p_f=p(h=h_f)=-p_c+p_{atm} \qquad (3b)$$

So the left hand side of Eq. (2), which is the pressure drop driving the flow in the tube, can be expressed using the boundary conditions as

$$p_0 - p_f = p_h + p_c \tag{4}$$

The capillary suction pressure p_c, applied at the top of the liquid column, can be obtained through the Laplace equation as

$$p_c = \frac{4\gamma\cos(\theta)}{D_c} \tag{5}$$

To estimate h_L in Eq. (2), we assume the flow to be laminar in the capillary tubes. So it can be estimated through the Darcy-Weisbach relation [31] as

$$h_L = f\frac{L_c}{D_h}\frac{u^2}{2g} \tag{6}$$

As the flow is laminar, so $f = 64/\mathrm{Re}$ where $\mathrm{Re} = \rho u D_h/\mu$. Use of this relation in Eq. (6) results in

$$h_L = \frac{32u\mu L_c}{\rho g D_h^2} = \frac{32\mu L_c}{\rho g D_h^2}\frac{dh_f}{dt} \tag{7}$$

where the average velocity in the capillary tube is related to the rate of the liquid column rise through $u = dh_f/dt$. Using Eqs. (4), (5) and (7) in (2) gives the final form of governing equation as

$$p_h + \frac{4\gamma\cos(\theta)}{D_c} = \frac{32\mu L_c}{D_h^2}\frac{dh_f}{dt} + \rho g h_f \tag{8}$$

If we neglect the gravity effects and take the imposed hydraulic pressure to be zero, then the first and last terms will vanish. Since $L_c = h_f$, an integration of the remaining equation leads to the well-known Washburn equation:

$$h_f = \sqrt{\frac{\gamma D_e\cos(\theta)}{4\mu}t} \tag{9}$$

Here D_e, the effective pore radius, is obtained through

$$D_e = \frac{D_h^2}{D_c} \tag{10}$$

For the general case when the gravity and hydraulic pressure are included, we use Eq. (8) to derive a relation between the location of liquid front h_f and time *t*. Using the schematic of the experimental setup shown in *Figure 1* and noting that $p_h = \rho g H$ and $h_f = L_c$, Eq. (8) can be rewritten as

$$\rho g H + \frac{4\gamma\cos(\theta)}{D_c} = \frac{32\mu h_f}{D_h^2}\frac{dh_f}{dt} + \rho g h_f \tag{11}$$

where h_f is the height of the liquid front. Note that we use the hydrostatic pressure inside the tube and burette to claim that 1) the externally imposed liquid pressure under the fritted glass is equal to the pressure in the burette on the same horizontal plane, 2) the corresponding burette pressure is $\rho g H$. If the fritted glass is saturated at the time of starting the test, a decrease in the volume of fluid within the burette can be related to an increase in the volume of fluid within the wipes through the equation

$$-\int_{H_0}^{H}\pi R_b^2 dH = \varepsilon_w\int_{L_p}^{h_f}\pi R_w^2 dh \tag{12}$$

where H_0 is position of fluid in the burette at the beginning of the test. Integration of Eq. (12) gives the relation between *H* and h_f as

$$H = H_0 - \varepsilon_w\left(\frac{R_w}{R_b}\right)^2(h_f - L_p) \tag{13}$$

Using Eq. (13) in Eq. (11) leads to

$$\lambda_1 - \lambda_3 h_f = \lambda_2 h_f\frac{dh_f}{dt} \tag{14}$$

where

$$\lambda_1 = p_s + \rho g H_0 + \rho g L_p\varepsilon_w\left(\frac{R_w}{R_b}\right)^2 \tag{15a}$$

$$\lambda_2 = \frac{32\mu}{D_h^2} \tag{15b}$$

$$\lambda_3 = \rho g\left(1 + \varepsilon_w\left(\frac{R_w}{R_b}\right)^2\right) \tag{15c}$$

Integration of Eq. (14) gives the final form of equation as

$$t = \frac{\lambda_2}{\lambda_3}\left[\frac{\lambda_1}{\lambda_3}\ln\left(\frac{\lambda_1}{\lambda_1 - \lambda_3 h_f}\right) - h_f\right] \tag{16}$$

For capillary model, we take $p_s = p_c$ in Eq. (15a) while using the Laplace equation for capillary pressure p_c from Eq. (5).

Darcy Model

We would now use an alternative approach where the wetted wipes behind the rising liquid front is assumed to be completely saturated, and will be modeled using the Darcy's law for single-phase flow in porous media. The flow of a liquid in an isotropic porous medium under isothermal conditions is governed by the Darcy's law

$$\tilde{V} = -\frac{K}{\mu}\tilde{\nabla}P \tag{17}$$

and continuity equation

$$\tilde{\nabla}\cdot\tilde{V} = 0 \tag{18}$$

where $\tilde{V}$ is volume averaged liquid velocity perpendicular to the wipe-plane and P is the pore averaged modified pressure. ($\tilde{V}$ and P are obtained after integrating the point-wise liquid velocity and pressure in an averaging volume several times bigger than the particles/fibers of a porous medium [32].) Though the wipes are likely to show anisotropic behavior, we will assume that direction of the liquid flow, which is perpendicular to the plane of the paper-like wipe, is one of the principal directions.

The modified pressure P is defined in such a way so as to include the effects of gravity induced liquid motion in a porous medium and is combined with the pore averaged hydrodynamic pressure p as

$$P = p + \rho g h \tag{19}$$

where h is the height of a point within a fully saturated (or fully wetted) porous medium. We would now model the motion of a liquid within a porous stack of wipes as shown in *Figure 1*. It is common to assume that the wipes below the rising liquid front are fully wet, i.e. all the pore spaces in the porous medium are occupied by the liquid after the liquid front pass them. For the one dimensional (1-D) fluid motion across the wipe-layer described in *Figure 1*, the Darcy's law, Eq. (17), and continuity equation, Eq. (18), reduce to

$$V = -\frac{K}{\mu}\frac{dP}{dh} \tag{20}$$

$$\frac{dV}{dh} = 0 \tag{21}$$

Combining Eq. (20) into Eq. (21), and noting that K and μ are constants, leads to an equation for pressure distribution in the wetted area as

$$\frac{d^2P}{dh^2} = 0 \tag{22}$$

Note that this equation is valid in the stack of wet wipe as well as in the porous fritted glass underneath it. (As shown in *Figure 1*, the fritted glass and the stack of wipes above it form a hybrid porous media where these two different porous media of distinct porosities and permeabilities are in series.) Integration of Eq. (22) results into a general solution of the form $P_p(h) = Ah + B$ where $0 \le h \le L_p$ and $P_w(h) = Ch + D$ where $L_p \le h \le h_f$. Note that P_p is modified pressure within the porous fritted glass and P_w is modified pressure within the stack of the wipes. The constants A ,B ,C and D are evaluated using the boundary conditions

$$p_p = p_{atm} + p_h \quad at \quad h = 0 \tag{23a}$$

$$p_w = p_{atm} - p_s \quad at \quad h = h_f \tag{23b}$$

$$p_w = p_p \quad at \quad h = L_p \tag{23c}$$

$$V_w = V_p \tag{23d}$$

that are in terms of the pore averaged hydrodynamic pressure p. Eqs. (23a) to (23c) can be transformed in terms of the modified pressure P as

$$P_p = p_{atm} + p_h \quad at \quad h = 0 \tag{24a}$$

$$P_w = (p_{atm} - p_s) + \rho g h_f \quad at \quad h = h_f \tag{24b}$$

$$P_w = P_p \quad at \quad h = L_p \tag{24c}$$

Use of the boundary conditions (24) and (23d) with the general solution of Eq. (22) results into the following expression for the modified pressure:

$$P_w(h) = \frac{\rho g(L_p - h_f) + p_s + p_h}{L_p(1-\frac{K_w}{K_p}) - h_f}h + p_{atm} - p_s + h_f\left(\rho g - \frac{\rho g(L_p - h_f) + p_s + p_h}{L_p(1-\frac{K_w}{K_p}) - h_f}\right) \tag{25}$$

Note that this solution is valid for $L_p \le h \le h_f$ with $P(h) = P_w(h)$; the front height h_f is a function of time. An expression for h_f can be derived by relating front speed dh_f/dt with the Darcy velocity [Eq. (20)] at front h_f as

$$\frac{dh_f}{dt} = \frac{V_w(h=h_f)}{\varepsilon_w} = -\frac{K_w}{\varepsilon_w \mu}\frac{dP_w}{dh}\bigg|_{h=h_f} \tag{26}$$

which through the use of Eq.(25) results in

$$\frac{dh_f}{dt} = -\frac{K_w}{\varepsilon_w \mu}\left(\frac{\rho g(L_p - h_f) + p_s + p_h}{L_p(1-\frac{K_w}{K_p}) - h_f}\right) \tag{27}$$

If the only external pressure is the hydrodynamic pressure, which based on *Figure 1* is $p_h = \rho g H$, then the governing equation for the front speed can be expressed as

$$\frac{dh_f}{dt} = -\frac{K_w}{\varepsilon_w \mu}\left(\frac{\rho g(L_p - h_f) + p_s + \rho g H}{L_p(1-\frac{K_w}{K_p}) - h_f}\right) \tag{28}$$

Using Eq. (13) in Eq. (28) to eliminate *H* leads to

$$\frac{dh_f}{dt} = -\frac{\lambda_1 + \rho g L_p - \lambda_3 h_f}{L_p(1-\frac{K_w}{K_p}) - h_f}\left(\frac{K_w}{\varepsilon_w \mu}\right) \tag{29}$$

where λ_1 and λ_3 are defined in Eqs. (15a) and (15c). Integration of Eq. (29) leads to following equation as an explicit relation between time and location of liquid front.

$$t = \frac{\varepsilon_w \mu}{K_w \lambda_3}\left[\left(\frac{\lambda_1 + \rho g L_p}{\lambda_3} - L_p(1-\frac{K_w}{K_p})\right)\ln\left(\frac{\lambda_1 + \rho g L_p}{\lambda_1 + \rho g L_p - \lambda_3 h_f}\right) - h_f\right] \tag{30}$$

If there was just one material (i.e. only the stack of wipes) present in the cylinder, then $L_p = 0$, and a comparison of Eqs. (30) and (16) under this condition gives a relation between the permeability and the hydraulic pore diameter as

$$K_w = \frac{\varepsilon_w}{32} D_h^2 \tag{31}$$

This implies that if this equation is satisfied, and the permeabilities of the fritted glass and wipes are the same (or if we had just one material instead of two), the predictions of both the Darcy's law based model and the Capillary model are identical.

Note that p_s is the suction pressure created at the liquid front. The suction pressure is a function of the porous-medium microstructure, liquid surface-energy, and dynamic contact angle. If the porous medium is composed of spherical beads, it is a function of beads radius [7]; if the porous medium is a fabric, there are some other expressions for suction pressure [6,12]. We propose a novel, more general expression to estimate the suction pressure in paper-based porous media as

$$p_s = \frac{\gamma \cos(\theta)}{M}\frac{1-\varepsilon}{\varepsilon} \tag{32}$$

where *M* is the ratio of volume and wetted surface-area of the particles in a porous medium. Details of derivation of Eq. (32) appear in appendix A.

Effect of Swelling of wipes

Most of the natural fibrous materials (such as cellulose) undergo swelling when a wetting liquid such as water comes in contact with fibers. It is generally accepted that crystallinity of wiping material plays a major role in the swelling process. The amount of water retained by swollen fibers varies from 6% to 100% of dry weight of fibers. This retained water causes an error in the capillary pore radius measurement, when it is measured by rising liquid method. It also affects the hydraulic pore-radius and permeability measurements [15].

Swelling starts with the wetting of fibers and ends on fibers reaching an equilibrium state. So it is a time related process that causes the wicking parameters of the wipes to vary in each location as the flow passes through the wipe. In the other words, the porosity, hydraulic pore radius, capillary pore radius[1], and permeability can said to be a function of time and spatial location within the porous wipes as a result of swelling.

[1] Capillary pore radius is the radius of capillary tube where the capillary (suction) pressure is generated when the dry tube comes in contact with a liquid, while the hydraulic pore radius is hydraulic radius of the capillary tube when flow of liquid happens in it under fully saturated conditions.

TABLE I. Properties of the test liquids

Type of liquid	Distilled water	Windex®
Density [Kg/m^3]	998	982
Viscosity [m Pa.S]	0.982	1.5
Surface tension [mJ/m^2]	72.8	27.65

EXPERIMENTAL STUDY

The experimental study of wicking into the wipes is divided into two sections: in the first section, wicking parameters of wipes and wetting liquids will be measured in the testing systems; in the latter section, the wicking in the test setup will be explained.

Cellulose wipes are commonly used in the household, medical and industrial applications. Two of the most important applications are paper towels and table napkins. We have chosen two different paper towels and a table napkin for this study. Water and cleaners are usually used as surfactants to clean the surfaces. We have used Windex®, a known common-use cleaner, and distilled water for this study. The reason for choosing distilled water instead of the regular tap water is that the chemical composition (and hence wettability) of different waters are not the same; so the results obtained with the water in a city may not be exactly the same as those obtained with the water from another city or country. So we have chosen to use distilled water to increase the repeatability of our test results. The characteristics of the liquids and wipes used in our experiments are presented in *Tables I and II*.

TABLE II. Characteristics of the wipes (the parameters are presented with the 95% confidence interval range [33]).

Designated name	A	B	C
Type of wipes	Paper towel	Paper towel	Table napkin
Brand Name	Bounty®	Scott®	Clarissa®
Cylinder radius R_w [m]	0.0155	0.0155	0.0155
Porosity of system ε	0.58	0.4	0.5
Parameter of M [μm]	47.9	53.3	35.8
Hydraulic radius of system R_h [μm]	14.6 ± 1.32	1.45 ± 0.7	2.5 ± 0.53
Permeability of system K [m^2]	$(1.55 \pm .4) \times 10^{-11}$	$(3.1 \pm 0.86) \times 10^{-13}$	$(4.0 \pm 0.48) \times 10^{-13}$

Measuring the Wicking Parameters

To compare the experimental results of wicking into wipes with the theoretical predictions, we need to measure some parameters used in the relations derived in sections 2.1 and 2.2. These parameters are: porosity of wipes (ε), permeabilities of the testing system (K) which includes the permeability of wipes (K_w) and that of the fritted glass (K_p), hydraulic pore radius of the testing system (R_h), capillary pore radius of wipes (R_c), surface tension of the liquids (γ), dynamic contact angle (θ), and suction pressure parameter (M). The experimental techniques for the testing materials and the results obtained are described briefly in this section.

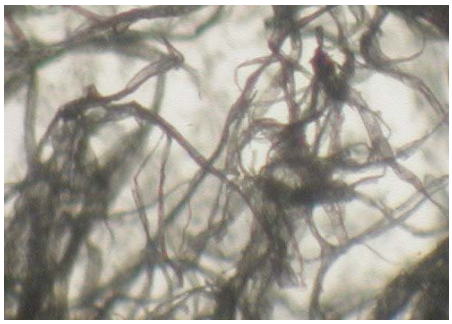

a) Micrograph for wipe A

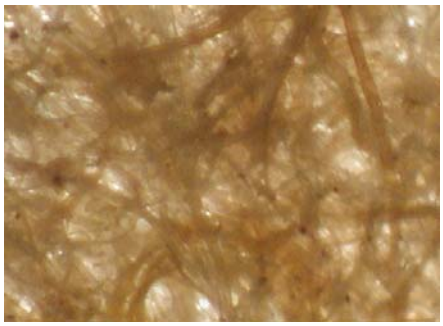

b) Micrograph for wipe B

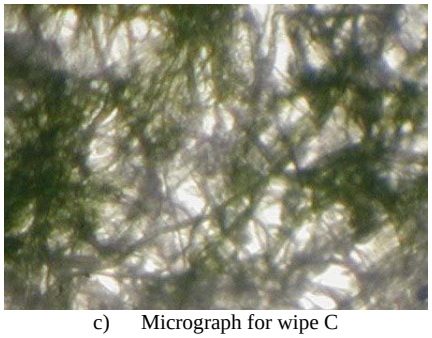

c) Micrograph for wipe C

FIGURE 3. Micrography of the structure of the wipes

Micrography

Micrographs of the wipes were prepared to study the microstructure visually (*Figure 3*). Micrography was also used to study changes in the wipe microstructure with the wetting of wipes. It was seen that the microstructure of wipe C shrinks more than the other wipes during wetting. It was also observed that the rate of change of the micro-structure due to wetting was quite high in wipe C (a few seconds to reach the equilibrium) in comparison to wipes A and B (a few minutes to reach the equilibrium).

Porosity

The mean porosity ε of wipes is defined as the ratio of liquid occupied pore volume to the total bulk volume. If Q_{sat} is the volume of liquid absorbed by a porous medium to saturate itself and Q_{tot} is its total volume in the dry state, then the porosity ε is given by

$$\varepsilon = \frac{Q_{sat}}{Q_{tot}} \tag{33}$$

Using dimensions shown in *Figure 1*, the expression for porosity changes to its final form

$$\varepsilon = \frac{Q_{sat}}{\pi R_w^2 L_w} \tag{34}$$

Permeability

We will now measure the permeability of system employed in the setup shown in *Figure 4*. We will impose a pressure on the wipe stack and measure the volume rate of the fluid passing through the wipes for such conditions. Here we will employ a well known method called the falling-head permeameter [7] to estimate the permeability. Assuming the system (wipes + fritted glass) to be fully saturated, we can employ Darcy's law for single-phase flows to get

$$V = \frac{K}{\mu}\frac{P}{(L_p + L_w)} \tag{35}$$

in which $P = p_h = \rho g H$ and K is the hybrid permeability of the system. The Darcy's velocity can be also be related to the falling liquid level (*Figure 4*) as

$$V = \frac{\pi R_b^2 \dfrac{dH}{dt}}{\pi R_w^2} \tag{36}$$

Combination of the above two relations results in

$$\frac{dH}{H} = \frac{K R_w^2 \rho g}{\mu (L_w + L_p) R_b^2} dt \tag{37}$$

On integrating Eq. (37) and using the initial condition $H(t=0) = H_0$, we get

$$\ln \frac{H_0}{H} = \frac{K \rho g R_w^2}{\mu (L_w + L_p) R_b^2} t \tag{38}$$

In a plot of $\ln(\frac{H_0}{H})$ versus time *t*, the slope of the trend line is equal to $\frac{K \rho g R_w^2}{\mu (L_w + L_p) R_b^2}$. Since all the other parameters in the slope are known, the permeability K can be estimated. For our experiments, each test was repeated four times to make sure that the slope of the line had a repeatable value. A sample trend line and its slope are presented in *Figure 5*, and the test results for various wipes are given in *Table 2*. The permeability measured was for the hybrid system consisting of the wipes and fritted glass. The method for estimating the permeability of the hybrid system is derived in detail in Appendix B.

Hydraulic pore radius

To measure the equivalent hydraulic pore-radius of the wipes + fritted glass system, we assume the hybrid system to consist of vertically aligned capillary tubes that are fully saturated. Based on Eq. (1), the fluid flow within wipes in the test setup shown in *Figure 4* can be written as

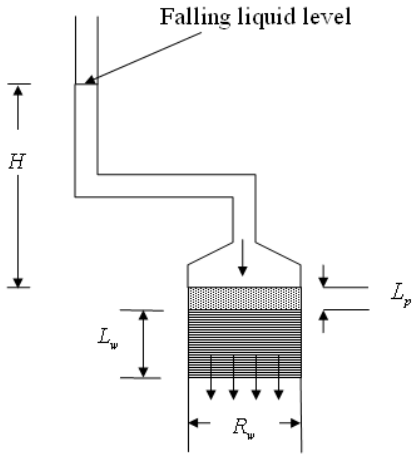

FIGURE 4. A schematic of the test-setup for measuring the permeability and hydraulic pore-radius of the hybrid system consisting of the fritted glass plate and stack of wipes

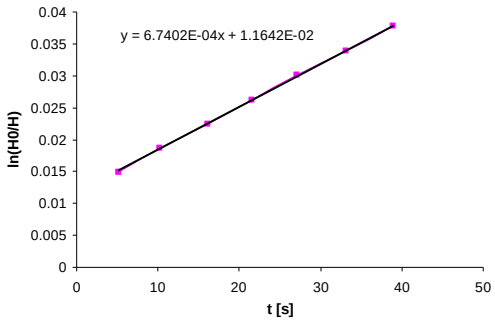

FIGURE 5. The fitted trend-line for the estimation of the permeability and hydraulic pore-radius in wipe C.

$$\frac{P_{up}}{\rho g} + h_{up} = \frac{P_{down}}{\rho g} + h_{down} + h_L \tag{39}$$

Noting that $h_{up} - h_{down} = L_p + L_w$, $P_{up} = P_h = \rho g H$, and $P_{down} = 0$, this equation can be simplified to

$$H = h_L - (L_p + L_w) \tag{40}$$

To estimate h_L in Eq. (40), once again we assume the flow to be laminar in the assumed homogenous capillary tubes and use the Darcy-Weisbach relation [31]:

$$h_L = f \frac{L_p + L_w}{D_h} \frac{u^2}{2g} \tag{41}$$

Here u is the average liquid velocity within the capillary tubes that can be estimated through the mass conservation law (i.e., the flow rate is related to the rate of depletion of liquid column in the burette):

$$u = \frac{-\pi R_b^2 \frac{dH}{dt}}{\varepsilon \pi R_w^2} \tag{42}$$

Substituting Eq. (42) in Eq. (41) and using the definition of friction factor f for laminar flow in the tubes to be $f = 64/\mathrm{Re}$ with $\mathrm{Re} = \rho u D_h / \mu$, we get following relation for the head loss within the porous medium.

$$h_L = -\frac{32 \mu R_b^2 (L_p + L_w)}{\rho g \varepsilon R_w^2 D_h^2} \frac{dH}{dt} \tag{43}$$

Substitution of Eq. (43) in Eq. (40), and the subsequent separation of variables leads to

$$\frac{dH}{H + L_p + L_w} = -\frac{\rho g \varepsilon R_h^2 R_w^2}{8\mu (L_w + L_p) R_b^2} dt \tag{44}$$

Integration of Eq. (44) and use of the initial condition $H(t=0) = H_0$ gives the final form of the equation as

$$\ln \frac{H_0 + L_p + L_w}{H + L_p + L_w} = \frac{\varepsilon R_h^2 R_w^2 \rho g}{8\mu (L_w + L_p) R_b^2} t \tag{45}$$

So in a plot of $\ln(\frac{H_0 + L_p + L_w}{H + L_p + L_w})$ versus time t, the slope of the fitted line is equal to $\frac{\varepsilon R_h^2 R_w^2 \rho g}{8\mu (L_w + L_p) R_b^2}$. Since all the other parameters in the slope are known through independent measurements, the hydraulic pore radius R_h can be found. The test results are given in *Table II*.

Capillary pore radius

To find a relation between the capillary and hydraulic pore radii, we used the definition of hydraulic radius as the ratio of net liquid volume inside capillary tubes to the wetted surface area of the tubes to formulate the expression for R_h as

$$R_h = \frac{N \pi R_c^2 h_f}{2 N \pi R_c h_f} \tag{46}$$

where R_c is capillary pore radius and N is number of longitudinal capillaries passing through the porous medium. Eq. (46) reduces to the following relation for estimating the capillary pore radius R_c .

$$R_c = 2 R_h \tag{47}$$

In our test, enough layers of wipes were stacked in the cylinder to enable us to measure the saturation height. Since the capillary pore radius is also related to the compression ratio[2] of the wiping material, we measured the density of wipes (i.e. number of the wipe layers in a unit length) in the cylinder during the test to maintain the same porosity and pore radius. To adjust the volume of the wipes to reach a desired wipe density, we used a special piston to compress them within the cylinder. The piston itself had a lot of pores in it, so the air could not be trapped under the piston as it was compressing the wipes.

[2] In compressible materials, the compression ratio is the ratio of their current volume under an external pressure to their initial volume under zero external pressure.

Contact angle and surface tension

The standard Wilhelmy plate method was used in a Dynamic Contact-angle Analyzer (DCA) to measure the surface tension of the testing liquid. The DCA was also used to measure the dynamic contact angles of the wipes and liquid system using the standard Wilhelmy plate method with a piece of flat rectangular paper replacing the metal plate. (To prevent the effect of absorption on the measuring angle, the testing sample was put into the liquid and was allowed to become fully saturated before the measuring of the contact angle.) The results of the surface tension and contact angle measurements are given in *Tables I and III*.

TABLE III. Contact angles of the wipe-liquid systems (with the 95% confidence interval range [33])

Type of liquid	Distilled water	Windex
Wipe A	55.9 ± 1.26	0
Wipe B	41 ± 0.71	0
Wipe C	$51. \pm 0.39$	0

Suction pressure parameter *M*

According to the newly proposed expression for the suction pressure as presented in Appendix A, the suction pressure parameter *M* is defined as the ratio of volume of particles/fibers in a porous medium to their wetted area (Eq. A-4). If we approximate the three-dimensional pore structure in paper as something generated by extruding a two dimensional micrograph along the vertical direction, this parameter can be equated to the ratio of the particle cross-sectional area to its perimeter. Thus we can use the micrographs of wipes given in *Figure 3* to estimate the value of *M* for each wipe after measuring the cross-sectional area and perimeter of solid portions of the micrographs. Note that if we assume the porous medium to be a fibrous material, the value of *M* would be equal to fiber radius. Therefore one of the effective ways of estimating *M* is to measure the average radius of fibers in the micrographs.

Measuring the Wicking Rate under Hydrodynamic Pressure

As we have mentioned before, the capillary pore radius is related to the compression ratio of wiping material, so to get accurate results we measured the density of each stack of wipes in the cylinder to make sure it is constant in all the tests for each of the wipes[3]. To adjust the volume of the wipes, a special piston was used to compress the stack of wipe layers within the cylinder (see *Figure 1*) to a desired height. At the start of each experiment, we have been saturating the fritted glass while the stacks of wipes were kept a few millimeters above the fritted glass. During the procedure, the end of the burette was closed to prevent the fluid from moving down. As the stack of wipes touch the fritted glass, the burette was opened to let the liquid move down the tube. A camcorder was used to record the height of liquid within the burette; the video film was reviewed later to extract the absorption rate into the wipes.

To make sure that our measurements were reliable, each test was repeated at least three times. We also did a scatter-estimation test on the wipe C to estimate the repeatability of the test results. *Figure 6* shows the results of scatter-estimation tests on wipe C with Windex; the measured 95% confidence intervals are shown with the help of the scatter bars. (This interval is a range of the measured quantity in which the measured value is expected to fall 95% of the times [33].) The small bars (especially till t = 6 sec) mean that our experiments were very repeatable. We are confident that all experiments listed in this paper show similar repeatability patterns. To get a good confidence level, it was necessary to avoid trapping of bubble under the fritted glass as the bubbles provide additional resistance to fluid moving upwards.

Similarly tests to measure wicking parameters (*Tables II and III*) were often conducted multiple times to obtain more than one measured values. The scatter in the property values thus obtained was once again quantified through the use of the 95% confidence interval.

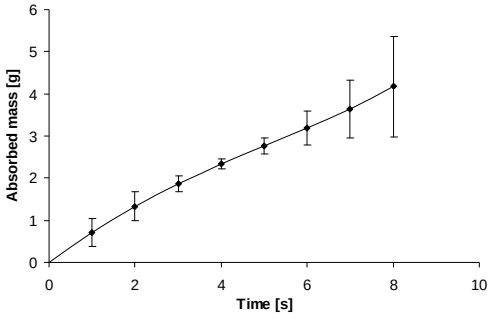

FIGURE 6. A scatter estimation on the wipe C with Windex experiment with scatter bars showing confidence interval of 95%

[3] Since the number of layers was high, we weighed the stack of wipes to make sure that we were using the same number of layers in different experiments with the same wipe. The precision of the microbalance used was 0.01 g which was less than the weight of a single layer. (The weight of layers for the test materials A, B, and C were 1.37 g, 2 g, and 1.37 g, respectively.) Using this method and such a microbalance, we ensured that the number of layers remained constant from test to test.

RESULTS AND DISCUSSIONS

Since we had an explicit relation for time in terms of the liquid front position in Eqs. (16) and (30), we gave different values of the liquid-front position h_f from zero to L_w, and then calculated the corresponding time for each position using the mentioned equations. The position h_f was then converted into the liquid mass absorbed into the wipes through the relation

$$m = \varepsilon_w \rho \pi R_w^2 (h_f - L_p) \qquad (48)$$

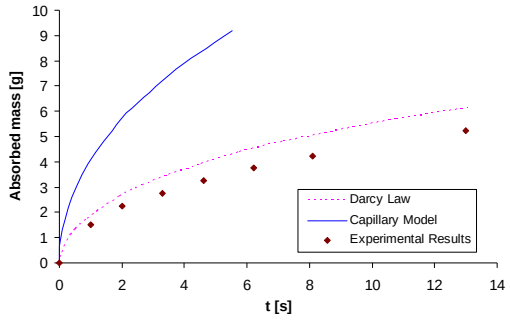

a) $p_h = 0$ *pa*

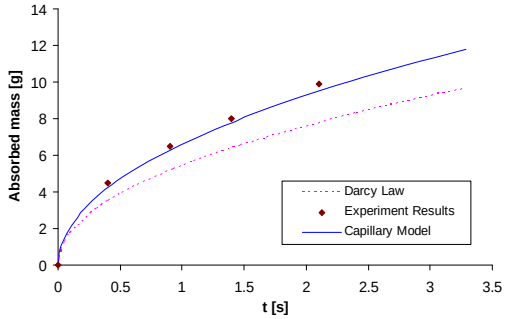

b) $p_h = 2683$ *pa* (H = 29 Cm)

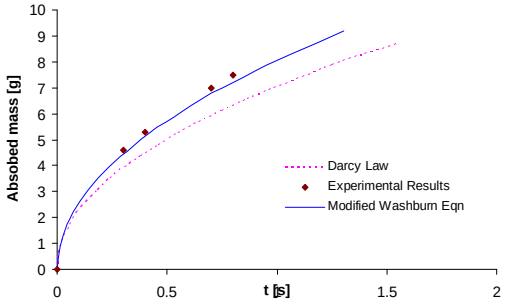

c) $p_h = 4758$ *pa* (H = 49 Cm)

FIGURE 7. Wicking rate in wipe A when water was used under three different externally-imposed liquid pressures.

As seen in *Figure 7*, the experimental and capillary model results are not close when the externally imposed liquid pressure is zero (*Figure 7a*). But as the externally imposed liquid pressure increases, the theoretical predictions obtained from the capillary model grow closer to the experimental measurements (*Figures 7b and 7c*). As for the Darcy law results, it has the opposite effect, i.e., there is an excellent prediction when the external pressure is zero. However, there is an increasing deviation from experiments with a rise in the external pressure. One possible reason for this progressive improvement of results for the capillary model is our method of measuring the hydraulic pore-radius. We measured this parameter while the materials were under the externally imposed liquid-pressure and as the imposed pressure compresses the material, the obtained parameters (permeability and hydraulic pore radius) are valid for the externally imposed liquid pressures equal to or close to the measuring pressure[4]. So we expect that as the difference between the measuring pressure[5] and testing pressure increases, the difference between the theoretical predictions and the experiment results would increase as well. This difference is more significant for those type materials that are more compressible or those that swell more as they get wet. This fact can explain why we have better theoretical results when an

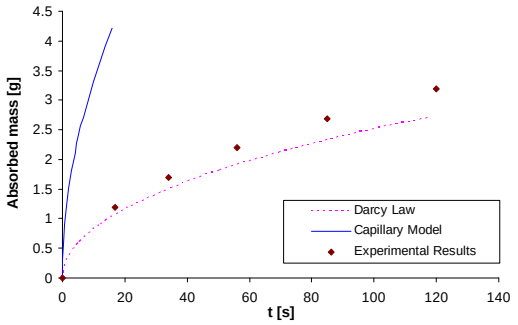

a) $p_h = 0$ *pa*

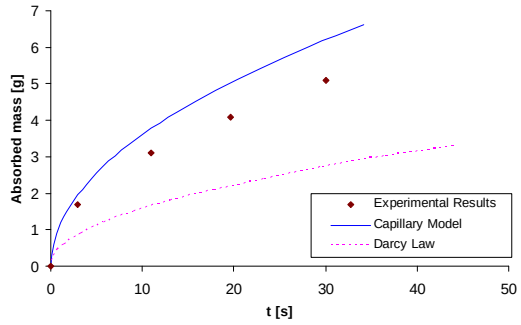

b) $p_h = 2683$ *pa* (H = 29 Cm)

[4] Note, we are dealing with compressible materials, so the externally imposed liquid-pressure compresses them and changes their wicking parameters.

[5] The externally imposed liquid-pressure at which the wicking parameters or wicking rate were measured

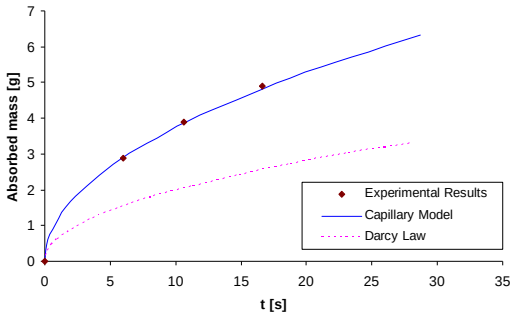

c) p_h = 4758 *pa* (H = 49 Cm)

FIGURE 8. Wicking rate in wipe B when water was used under three different externally-imposed liquid pressures.

external liquid pressure is imposed during wicking.

In *Figure 8*, we have used another type of paper towel with its compressibility lower than that of type A. As we can see in *Figure 8a*, theoretical results predicted using the capillary model for the case of pure wicking (no externally imposed liquid pressure) are way off the target once again, in fact more than the one seen for wipe A in *Figure 7*. So one might surmise that as the compressibility of wipes decreases, the accuracy of the capillary model predictions deteriorates for the pure wicking case. Theoretical predictions by the Darcy's law model are good as before for this case. However tables are turned as the external pressure is increased: performance of the capillary model improves while predictions of the Darcy's-law based model deteriorate. In fact the former gives a very accurate prediction in part (C) of *Figure 8*, while the latter under-predicts the absorbed mass.

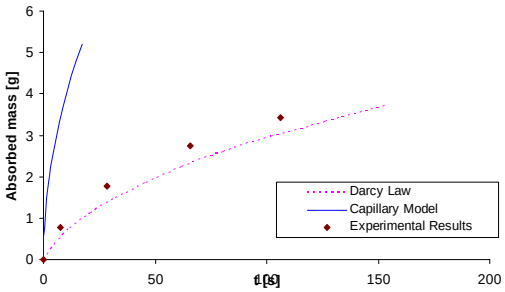

a) p_h = 0 *pa*

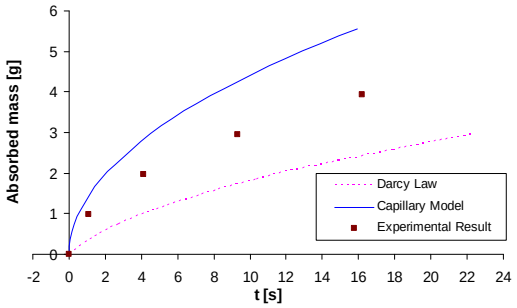

b) p_h = 2683 *pa* (H = 29 Cm)

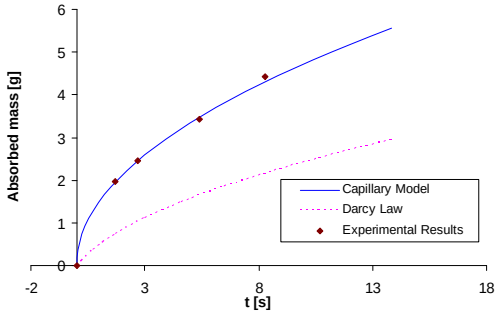

c) p_h = 4758 *pa* (H = 49 Cm)

FIGURE 9. Wicking rate in wipe C when Windex was used under three different externally-imposed liquid pressures.

Figure 9 shows the results obtained for wipe C, a table napkin. In addition to having a higher compressibility, the napkins also swelled faster than the paper towel as they got wet. Again we can see a very large difference between the capillary model predictions and the experiment for the zero imposed pressure or pure wicking case (*Figure 9a*). Once again Darcy law predictions are quite accurate. However as the external pressure increases, predictions of the capillary model improve and approach the experimental results (*Figures 9b and 9c*); Darcy's law model predictions deteriorate as before.

It is clear from *Figures 7, 8 and 9* that for wicking (of both the free and pressurized types) in swelling materials such as paper napkins and towels, the capillary and Darcy's law based models fail to perform consistently over the whole range of imposed pressures. For the lower imposed pressures, the Darcy's law based models perform better where as for the higher imposed pressures, the capillary model are more accurate. This is in contrast to their sterling behavior in predicting wicking accurately in rigid polymer wicks [7, 14]. The reason could lie in the fact that the measurement of certain wicking parameters (such as the hydraulic pore-radius, the wicking parameter *M*, and the permeability) may be affected by swelling of the cellulose-based porous

medium. Experiments have shown that swelling of cellulose has a time-scale that matches the time-scale of the wicking process, so some wicking parameters in such materials might be a function of time and the location of liquid front in addition to other usual factors. As a result, the conventional methods for measuring wicking parameters, which rely on establishing steady-state conditions in porous media before the start of measurement, may not be valid for swelling materials. In other words, the measured wicking parameters are expected to be reliable only when they are used at liquid pressures that are close to the imposed pressure used during the measurement.

Saturation time, which could be defined as the time needed for a liquid to make the stack of wipes fully wet or saturated, was measured next. Such a time could be measured from the recorded video films of the aforementioned wicking experiments. However since the volumes of liquid needed to make wipes fully wet were different for the three wipes, we defined a special fixed volume (which was less than the saturation volume for the least absorbent type of the testing wipes) to compare the absorption time. So, the time needed for each wipe to absorb a defined volume of selected liquids were measured and compared together to see how the hydrodynamic pressure may affect the absorption time in each of the tested wipes. (Note that since our theoretical approaches did not predict the experimental results consistently well, we have used only the experimentally measured saturation-times of the three tested wipes.)

The effect of the externally imposed liquid-pressure on the absorption time for the three tested wipes is shown in *Figure 10*. It shows that as the imposed pressure increases, the effect of the capillary pressure grows less important in comparison to the imposed pressure; this is why we can see a convergence of the lines in *Figure 10* with an increase in the imposed pressure. The pattern is repeated in both *Figures 10a and 10b* although the absorption time for Windex is more than that for the water. The changing of the test liquid merely changes the speed of absorption, but leaves the pattern of liquid absorption unchanged. Of course, some physical or chemical properties of the liquids (such as the polarity or chemical reactivity) and the solid-liquid interactions are different in the two cases, which consequently lead to minor differences in the absorption pattern. It might be the cause of a slight difference seen between *Figures 10a and 10b*.

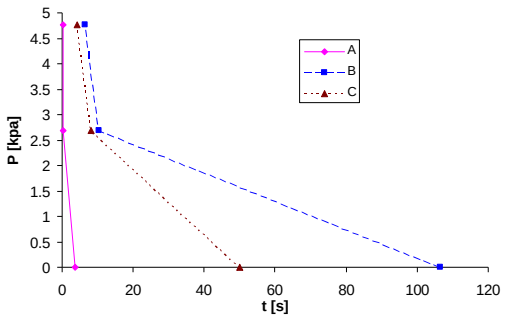

a) Test liquid is water

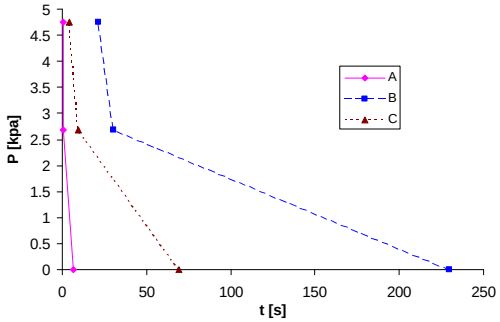

b) Test liquid is Windex

FIGURE 10. The effect of externally imposed liquid pressure on the absorption time for wipes A, B and C when the three wipes absorbed the same volume of liquid

In *Figure 11*, the change in the absorption times for each wipe are presented for the two test-liquids separately to show the effect of changing liquid properties on the absorption rate. The pattern of the liquid absorption is similar for both the liquids in

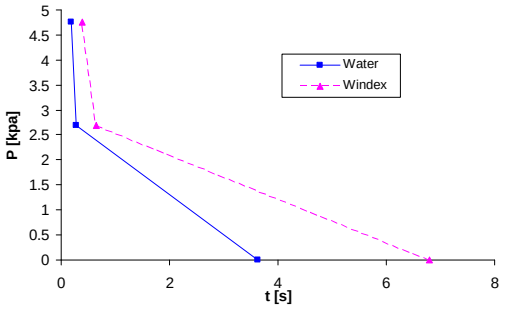

a) Wipe A

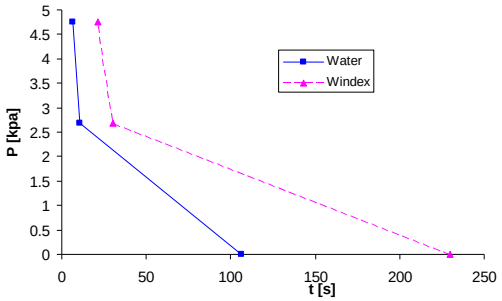

b) Wipe B

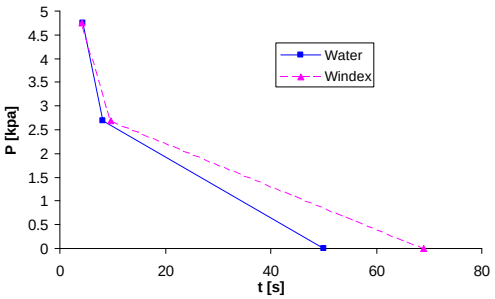

c) Wipe C

FIGURE 11. The effect of externally-imposed liquid pressure on the absorption times for wipes A, B and C when the three wipes absorbed the same volume of liquid

wipes A and B (*Figures 11a and 11b*) while there is a difference for wipe C (*Figure 11c*). It shows that when the liquid was switched in wipes A and B, the structural interaction between the new liquid and wipe matrix was less than that in wipe C. All of the plots in *Figures 10 and 11* show that as the externally imposed liquid-pressure increases, it enhances the absorption rate. But the effect of increasing the imposed pressure from zero to 2683 kpa is much higher than the effect of increasing it from 2683 kpa to 4758 kpa. For example, in wipe A with water, when the imposed pressure increases from zero to 2683 kpa, the saturation time decrease from 3.63 to 0.27 seconds, which means a decrease of 93 percents. On the other hand, increasing the imposed pressure from 2683 kpa to 4758 kpa (77 percent increase) decreases the saturation time from 0.27 to 0.19 seconds, which is merely 2.2 percent of its initial saturation time of 3.63 seconds. This important result shows that as the externally imposed liquid pressure increases, its relative effect on the absorption rate (or the wicking rate) decreases.

To consolidate the above argument, two non-dimensional parameters of 'relative pressure' and 'relative absorption time' are proposed:

$$P_{re} = \frac{p_c + p_h}{p_c} \qquad (49a)$$

$$T_{re} = \frac{time \quad of \quad saturation \quad when \, P = p_c + p_h}{time \quad of \quad saturation \quad when \, P = p_c} \qquad (49b)$$

Figure 12 shows our previous point about the effect of the externally imposed liquid pressure. It shows that as the relative pressure P_{re} increases, the change in the relative time T_{re} decreases. This effect is more significant in wipes B and C than wipe A. In other words, both *Figures 11 and 12* show that as the imposed pressure increases, its ability to decrease the absorption time decreases. A speculative explanation of this phenomenon can be attempted as follows. When an externally applied liquid-pressure is imposed on the wipes, it compresses them and reduces their pore sizes, which in turn lead to two effects: 1) increase in the capillary suction pressure, 2) decrease in the permeability (or increase in flow resistance) of wipes. During the first increase in P_{re} perhaps the first effect is dominant, and as a result, increase in the applied pressure as well as the capillary pressure provide higher motive force to the wicking liquid and thus cause the saturation times to decrease. During the second increase in P_{re} perhaps the second effect is dominant, and the increase in the motive force due to an increased capillary pressure is cancelled by an increase in flow resistance, and as a result, the saturation time does not decrease as much.

In conclusion, we would like to mention that some wicking tests were also conducted with a special 'microfiber' wipes that were characterized by the presence of microscopic apertures to enhance wicking. However significant scatter in the absorbed-mass-vs-time plots were observed for this wipe. It was postulated that presence of microscopic apertures rendered the wipe microstructure a dual-scale porous medium (i.e. large lengths-scale apertures coexisting with much smaller length-scale pores); so if the apertures aligned during the stacking of wipes, wicking behavior was completely different from when the apertures were not aligned. As a result, it was felt by the authors that more study is needed to develop a reasonable theoretical model for wicking in such dual-scale wipes, and such an effort will be undertaken in future.

SUMMARY AND CONCLUSION

Wicking of liquid under externally imposed liquid pressure into three cellulose wipes is studies experimentally and theoretically. The wicking and wetting parameters of testing wipes were measured to

enable a comparison between theoretical predictions and experimental results. Wicking models based on

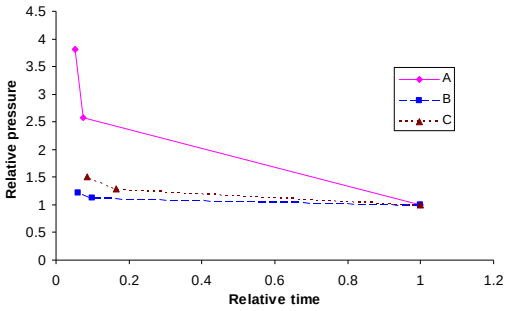

a) Test liquid is water

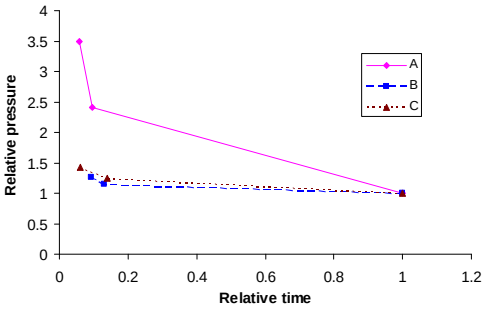

b) Test liquid is Windex

FIGURE 12. The effect of externally-imposed liquid pressure on the absorption time when absorbing a fixed volume of liquid (using the non-dimensional pressure and time for wipes A, B and C)

Darcy law and aligned capillary tubes were developed as our theoretical models. A new formula for prediction of suction pressure is presented, which is based on the ratio of mean values of volume and wetted surface-area of particles in the porous medium. It was seen that the predictions of the capillary model and Darcy law based models were not consistent over the whole range of the externally applied liquid pressure during wicking: the capillary model was accurate at higher applied pressures while the Darcy law based model was better at zero pressure (pure wicking) situations. The cause of this inconsistency may be that the wicking parameters may be affected by the applied pressure in compressible wipes as well as change during the wetting of cellulose-based paper wipes. It also was seen that as the applied pressure increases, its relative effect on the absorption rate of saturation time decreases.

ACKNOWLEDGEMENT

The authors are grateful to Dr. Andrei Skliarov and Dr. Steve Hardcastle for their help in preparing the test materials and experimental setup.

NOMENCLATURE

D_c	Capillary pore diameter
D_h	Hydraulic pore diameter
D_e	Effective pore diameter
f	Friction factor in Darcy-Weisbach relation [Eq. (6)]
g	Acceleration due to gravity
H	Height of liquid column in the burette [*Figure1*]
H_0	Initial height of liquid in the burette [*Figure 1*]
h	Vertical coordinate or elevation in *Figures 1 and 3*
h_f	Height of the liquid front in the wipes
h_0	Initial height of the liquid front ($h_0 = h_f(t=0)$)
h_{up}	Height of the upper surface in the hybrid system of fritted glass +stack of wipes [*Figure 3*
h_{down}	Height of the lower surface in the hybrid system of fritted glass +stack of wipes [*Figure 3*]
h_{ss}	Final steady-state height of the liquid front in the wipe.
h_L	Head loss in the capillary tube
K	Hybrid permeability of the fritted glass + stack of wipes system
K_p	Permeability of the porous fritted glass
K_w	Permeability of the stack of the wipes
L_p	Thickness of the fritted glass [*Figure 1*]
L_w	Thickness of the stack of wipes in the cylinder [*Figure 1*]
L_c	The wetted length of the capillary tubes through which the fluid is passing
M	The suction pressure parameter, which is the ratio of volume and surface area of solid particles [Eq. (A-4)]
m	Absorbed liquid mass
p	Pore averaged liquid pressure
P	Pore averaged modified pressure [Eq. (19)]
p_0	Pressure in capillary tubes at height $h = h_0$
p_f	Pressure in capillary tubes at liquid front [$h = h_f$]
p_c	Capillary pressure [Eq. (5)]
p_s	Suction pressure at liquid front
p_h	Hydraulic pressure [$\rho g H$]
p_p	Pressure inside the porous fritted glass
p_w	Pressure inside the stack of the wipes
p_{up}	Pressure on the hybrid system of fritted glass +stack of wipes [*Figure 3*]
p_{down}	Pressure below the hybrid system of fritted glass +stack of wipes [*Figure 3*]
P_{re}	Relative pressure [Eq. 49a]
p_{atm}	Atmospheric pressure
Q_{tot}	Total volume of a porous medium
Q_{sat}	Volume of the fluid needs to saturate a porous medium
R_h	Hydraulic radius
R_c	Capillary pore radius
R_b	Burette radius
R_w	Cylinder (wipe) radius
Re	Reynolds number
T_{re}	Relative time [Eq. 49b]
t	Time
u	Speed of fluid flow in the capillaries
u_0	Speed of fluid flow in the capillary tubes in the

	height $h = h_0$
u_f	Speed of fluid flow in the capillary tubes at liquid front $h = h_f$
V	Volume averaged Darcy velocity
V_p	Darcy velocity in the fritted glass
V_w	Darcy velocity in the stack of the wipes
$\tilde{V}$	Volume averaged Darcy velocity in vector form
$\lambda_{1,2,3}$	Parameters [defined in Eqs. 15a,b,c]
ε	Composite porosity of the wipes + fritted glass system
ε_w	Porosity of wipes
ρ	Density of a liquid
γ	Surface tension of a liquid
θ	Contact angle
μ	Viscosity of a liquid

REFERENCES

[1] Lucas, R,; Rate of Capillary Ascension of Liquids; *Kollid* Z.; 1918, 23, 15.

[2] Washburn, E.V.; The Dynamics of Capillary Flow; *Phys. Rev*. 1921, 17, 273.

[3] Sutera, S.P.; The history of Poiseuille's law; *Annual Review of Fluid Mechanics;* 1993, 25, 1-19.

[4] Szekely, J.; Neumann, A.W.; and Chuang, Y.K.; The Rate of Capillary Penetration and the Applicability of the Washburn Equation; J. *Colloid Interface Sci*; 1971, 35, 273-278.

[5] Bear, J.; Dynamics of Fluids in Porous Media; Elsevier Science; 1972.

[6] Pillai, K.M.; and Advani, S.G.; Wicking Across a Fiber-Bank; J. Colloid and Interface Sci; 1996, 183, 100-110.

[7] Masoodi, R.; Pillai, K.M.; and Varanasi, P.P.; Darcy's Law based Models for Liquid Absorption in Polymer Wicks; J. AIChE; 2007, 53, 11, 2769-2782.

[8] Chwastiak, S.A.; Wicking Method for Measuring Wetting Properties of Carbon Yarn; J. Colloid Interface Sci.; 1973, 42, 298-309.

[9] Scher, K.E.; Master's Thesis; Dept. of Chemical Engineering; University of Washington; 1983.

[10] Hodgson, K.T. and Berg, J.C.; The Effect of Surfactants on Wicking Flow in Fiber Networks; J. Colloid Interface Sci.; 1988, 121, 1, 22-31.

[11] Fowkes, F.M.; Role of Surface Active Agents in Wetting; J. Phys. Chem.; 1953, 57, 98-103.

[12] Williams, J.G.; Morris, C.M.; and Ennis, B.C.; Polym. Eng. Sci.; 1979,14, 6, 413-419.

[13] Kim, S.H.; Lee, J.H.; and Lim, D.Y.; Dependence of Sorption Properties of Fibrous Assemblies on their Fabrication and Material Characteristics; Tex. Res. J.; 2003, 73, 5, 455-460 .

[14] Masoodi, R.; Pillai, K.M.; and Varanasi, P.P.; Role of Hydraulic and Capillary Radii in Improving the Effectiveness of Capillary Model in Wicking; ASME Summer Conference; Jacksonville, FL, USA; August 10-14, 2008.

[15] Chatterjee, P.K. and Gupta, B.S.; Absorbent Technology; Amsterdam; Elsevier; 2002.

[16] Pan, N. and Gibson. P.; Thermal and Moisture Transport in Fibrous Materials; Cambridge; Woodhead; 2006.

[17] Zhong, W.; Ding, X.; and Tang, Z.L.; Modeling and Analyzing Liquid Wetting in Fibrous Assembles; Textile Res. J.; 2001, 71, 9, 762-766.

[18] Zhong, W.; Ding, X.; and Tang, Z.L.; Analysis of Fliud Flow Through Fibrous Structures; Textile Res. J.; 2002, 72, 9, 751-755.

[19] Lukas, D.; Soukupova, V.; Pan, N; and Parikh, D.V.; Computer Simulation of 3-D Liquid Transport in Fibrous Materials; Simulation; 2004, 80, 11, 547-557.

[20] Patnaik, A.; Rengasamy, R.S.; Kothari, V.K.; and Ghosh, A.;. Textile Progress; Woodhead; 2006, 38, 1, 1-105.

[21] Pan, N. and Zhong, W.; Fluid Transport Phenomena in Fibrous Materials; Textile Progress; Woodhead; 2006, 38, 2, 1-93.

[22] Young, T.; An essay on the cohesion of fluids; Philos. Trans. R. Soc.; 1805; London, 95, 65-87.

[23] Berg, J.C.; Wettability; New York; Marcel Dekker; 1993.

[24] Dussan, E.B. and Davis, S.H.; On the Motion of a Fluid-Solid interface Along a Solid Surface; J. Fluid Mech.; 1974, 65, 71-95.

[25] Dussan, E.B.; On the Spreading of Liquids on Solid Surfaces; Static and Dynamic Contact Lines; Ann. Rev. Fluid Mech.; 1979, 11, 371-400.

[26] Ghali, K.; Jones, B.; and Tracy J.; Experimental Techniques for Measuring Parameters Describing Wetting and Wicking in Fabrics; Textile Res. J.; 1994, 64, 2, 106-111.

[27] Li, Z.; Giese, R.F.; Van Oss, C.J.; Kerch, H.M.; and Burdette, H.E.; Wicking Techniques for Determination of Pore Size in Ceramic Materials; J. Am Ceramic Soc.; 1994, 77, 8, 220-22.

[28] Bachmann, J.; Woche, S.; Goebel, M.O.; Kirkham, M.B.; and Horton, R.; Extended Methodology for Determining Wetting Properties of Porous Media; Water Resources Res.; 2003, 39, 12, 1353.

[29] Nagy, V. and Vas, L.M.; Pore Characteristic Determination with Mercury Porosimetry in Polyester Staple Yarns; Fibers & Textiles in Eastern Europe; Jul/Sep 2005, 13, 3, 21-26.

[30] Dang-Vu, T. and Hupka, J.; Characterization of Porous Materials by capillary Rise Method; Physicochemical Problems of Mineral Processing; 2005, 39, 47-65.

[31] Cengel, Y.A. and Cimbala, J.M.; Fluid Mechanics Fundamentals and Applications; McGraw-Hill, 2006, 329-331.

[32] Tucker, C.I. and Dessenberger, R.B.; Governing Equation for Flow and Heat Transfer in Stationary Fiber beds; In: SG Advani. Flow and Rheology in Polymer Composites Manufacturing; Elsevier Science; 1994; Ch8.

[33] Wheeler, A.J. and Ganji, A.R.; Introduction to Engineering Experimentation; Prentice Hall, 1996.

APPENDIX A

Derivation of Expression for Suction Pressure

Here in order to find the suction pressure, we apply the energy balance principle to wicking. The amount of energy needed to raise the liquid in porous medium is equal to the sum of the viscous energy dissipated by the fluid, the energy spent on accelerating the fluid from zero to the wicking speed, and the energy needed to overcome the gravity. The inertial energy can be neglected as the speed of liquid is very low. We also neglect the gravity effects at this stage because we can include it later in the Darcy's law. So the reduction of free surface energy is equated to the viscose dissipation energy when the liquid moves within the porous medium. As the liquid moves through the porous medium, it reduces the dry surface area and so increases the wetted surface area. If γ_s stands for surface energy in dry surface and γ_{sl} stands for surface energy in wetted surface areas, then viscous dissipation energy will be

$$(\gamma_s - \gamma_{sl})dA = -dw_v \qquad \text{(A-1)}$$

in which dA is interfacial area and w_v is viscous work done during the flow of the liquid.

According to Young's equation, the relation between the contact angle and surface energy is given by

$$\cos\theta = \frac{\gamma_s - \gamma_{sl}}{\gamma} \qquad \text{(A-2)}$$

in which γ is represents the surface energy of the liquid and θ is contact angle. Combination of Eq. (A-1) and Eq. (A-2) leads to the following expression for viscous dissipation energy.

$$-dw_v = \gamma \cos\theta dA \tag{A-3}$$

If V_s and A are the volume and surface area of solid particles, let us define the suction pressure parameter M as

$$M = \frac{V_s}{A} \tag{A-4}$$

which leads to the following expression for change in surface area:

$$dA = \frac{dV_s}{M} \tag{A-5}$$

If we approximate the three-dimensional pore structure in paper as something generated by extruding a two dimensional micrograph (as shown schematically in *Figure A-1*) along the vertical direction, M can be equated to the ratio of the particle cross-sectional area to its perimeter. Hence V_s can be related to porosity through

$$dV_s = A_{cs}\, dh\, (1-\varepsilon) \tag{A-6}$$

where A_{cs} is the cross-sectional area of the porous medium perpendicular to the fluid flow velocity. Combination of Eqs. (A-5) and (A-6) leads to the following expression for interfacial surface area:

$$dA = \frac{A_{cs} dh(1-\varepsilon)}{M} \tag{A-7}$$

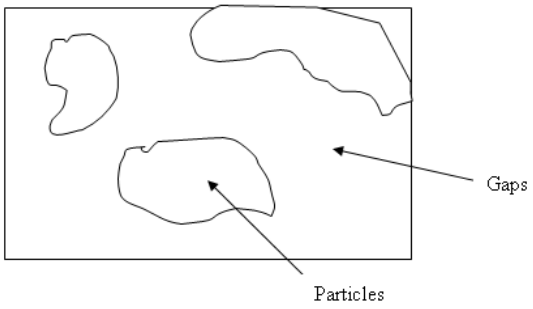

FIGURE A-1. A schematic of particles and void areas in the cross-section of a porous medium.

We assumed M stays constant during the wetting which is valid if change in the size of particles/fibers is small along the thickness direction. Substituting dA from Eq. (A-7) into Eq. (A-3) gives the final form of dissipation energy as

$$-dw_v = \gamma \cos\theta \frac{A_{cs} dh(1-\varepsilon)}{M} \tag{A-8}$$

The mechanical work needed to move the fluid by dh is

$$dw_m = F_p\, dh \tag{A-9}$$

where F_p is the pulling force that 'pulls' the liquid front through the porous medium. As per the definition of suction pressure, this pulling force should be equal to $p_s.\varepsilon A_{cs}$. So we can write

$$dw_m = p_s \varepsilon\ A_{cs} dh \tag{A-10}$$

As per energy balance, the total energy of system after moving the front liquid into the porous medium should be equal to its initial zero value. So the summation of the left sides of Eqs (A-8) and (A-10) should be zero, i.e. $dw_v + dw_m = 0$. The resultant final expression for the suction pressure is

$$p_s = \frac{\gamma_l \cos(\theta)}{M} \frac{1-\varepsilon}{\varepsilon} \tag{A-11}$$

APPENDIX B

Permeability of a Hybrid System

We have measured the permeability of the hybrid (wipes + fritted glass) system in our test setup using the falling head permeameter. However in order to estimate the permeability of only the wipes, the hybrid system will be treated as two porous media that are in series as follows.

First we measure the permeability of porous fritted glass (K_p) and hybrid system (K) separately using the falling head permeameter described in section 3.1.3. If K_w is designated as the permeability of the stack of wipes, L_w is the length of the wipe stack in the cylinder and L_p is the length of porous fritted glass (see *Figure 1*.), then Darcy's law will lead to:

$$Q = \frac{K}{\mu} \frac{\Delta P}{L} \tag{B-1}$$

where Q is flow rate, ΔP is steady state pressure drop occurring in the hybrid system, and L $(= L_p + L_w)$ is the total length of composite system. As the flow rates within the porous fritted glass and the wipe stack are the same, so

$$Q = \frac{K_w}{\mu} \frac{(\Delta P)_w}{L_w} = \frac{K_p}{\mu} \frac{(\Delta P)_p}{L_p} \tag{B-2}$$

Note that the total pressure loss ΔP will be equal to the summation of the individual pressure drops in the both media:

$$(\Delta P)_w + (\Delta P)_p = \Delta P \tag{B-3}$$

If the pressure drop terms from Eqs (B-1) and (B-2) are put into Eq. (B-3), we get

$$\frac{L_w}{K_w} + \frac{L_p}{K_p} = \frac{L_w + L_p}{K} \tag{B-4}$$

So the overall hybrid permeability K is the harmonic mean of the two constituent permeabilities, K_w and K_p. From Eq. (B-4) the final expression for the permeability of wipes K_w is

$$K_w = \frac{L_w K_p K}{(L_w + L_p)K_p - L_p K} \tag{B-5}$$

AUTHORS' ADDRESSES

KRISHMA M. PILLAI, Ph.D.
REZA MASOODI, Ph.D.
Laboratory for Flow and Transport Studies in Porous Media
Deaprtment of Mechanical Engineering
Univeristy of Wisconsin-Milwaukee
3200 N. Cramer Street
Milwaukee, WI 53211

PADMA P. VARANASI, Ph.D.
Waukesah Electric Systems
400 S. Prairie Avenue
Waukesha, WI 53186